GUIDE TO THE ZARELAB

July 2009 **Department of Chemistry, Stanford University**

Welcome to the ZARELAB.

This booklet has been prepared to make your visit with us more rewarding by presenting a survey of our recent research activities. Each section was written by those members pursuing the work described therein.

Please feel free to ask my lab manager, Dr. David Leahy, or any other members of my group to discuss any project.

On page 17 is a list of all members of the Zare group as of June 15, 2009 and information on how to contact them. On pages 18 through 20 are floor plans of offices and labs in the Mudd Building and the Clark Center. The last pages show maps of the Stanford campus and its vicinity.

Do enjoy your visit!

Richard N. Zare

Dick Zare and the rocket test.

INSIDE THIS GUIDE

TABLE OF CONTENTS

$H + H_2$ Reaction Dynamics

Nate Bartlett, Justin Jankunas

Following an over thirty-year history of gas phase reaction dynamics in the Zarelab, we continue the study of $H + H_2$ reaction. Indeed, it is a very exciting time for our section as ample experimental results and theoretical knowledge allow us to start contemplating ever more complex experiments.

Using a home-built three-dimensional ion imaging experimental apparatus[1] we were previously able to study reactive and inelastic scattering in an $H + H_2$ reaction and its isotopic analogues. We did this by using a tunable photolysis of HBr in the HBr/D_2 mixture. This generated fast H atoms that then went on to scatter either reactively or inelastically off D_2, to give HD (v'=1,3, j') or D_2 (v'=1-4, j'), respectively. The products of interest were state-selectively ionized using [2+1] resonance-enhanced multiphoton ionization (REMPI). The resulting ions were accelerated toward a multichannel plate (MCP) coupled to a delay-line anode which measures the three-dimensional velocity distribution of the reaction products which can then be converted to a differential cross section using the PhotoLOC (photoinitiated reaction analyzed with the law of cosines) technique developed in the Zarelab.

The experimental results on reactive scattering in an $H + D_2 \rightarrow HD$ (v'=1, j') + D reaction agreed well with the theoretical predictions.[2] As expected, we found two different reaction channels if the spin-orbit coupling in Br is taken into account. Also, as the rotational excitation of HD increased the differential cross sections (DCSs) shifted from backward to sideward scattering, again in an agreement with the theoretical predictions. $H + D_2 \rightarrow HD$ (v'=3, j') + D reaction exhibited an even richer dynamics.[3] In particular, time-delayed forward scattering was attributed to a glory effect that resulted from a near- and far-side quantum interference. Inelastic scattering experiments also revealed a few interesting features.[4] It was shown, for example, that the translational H atom energy was transformed into a vibrational D_2 energy mainly via a bond elongation with forward scattered products rather than bond compression and backward scattered products.

We are actively working towards the goal of using aligned samples of D_2 as scattering targets in the $H + D_2$ reaction. It has been theoretically shown that reactant polarization can greatly alter the chemical reactivity.[5] As a first step we have used stimulated Raman pumping to prepare highly aligned and oriented samples of H_2, HD and D_2 under collision-free conditions.[6] We have prepared both, states which undergo time-dependent rotational depolarization due to coupling between the rotational and nuclear spin angular momenta, and those that do not. The time-dependent rotational polarization was interrogated using polarized [2+1] REMPI for pump-probe delay times of up to 13 μs, about 10 times longer than has ever been measured with this method. We found that the calculated depolarization and our experimental data were in excellent agreement (see figure below). States for which no depolarization occurs we found that the prepared samples retained their initial degree of alignment for at least up to 8 μs, about 1000 times longer than what will be required for the use in a chemical reaction. This gives us confidence to further pursue our goal to use an aligned D_2 molecule in a scattering study. Finally, we are also very eager in testing the geometric phase effects predicted theoretically[7] for an $H + H_2$ reaction: an experiment that would truly push the limits of our understanding of the simplest bimolecular reaction as well as make us (re)think of how good our experimental apparatus really is!

[1] K. Koszinowski, N. T. Goldberg, A. E. Pomerantz, and R. N. Zare, *J. Chem. Phys.* **125**, 133503 (2006).

[2] K. Koszinowski, N. T. Goldberg, J. Zhang, R. N. Zare, F. Bouakline, and S. Althorpe, *J. Chem. Phys.* **127**, 124315 (2007).

[3] N. T. Goldberg, J. Zhang, D. J. Miller, and R. N. Zare, *J. Phys. Chem. A* **112**, 9366 (2008).

[4] N. T. Goldberg, J. Zhang, K. Koszinowski, F. Bouakline, S. Althorpe, and R. N. Zare, *PNAS* **105**, 18194 (2008).

[5] J. Aldegunde, M. P. de Miranda, J. M. Haigh, B. K. Kendrick, V. Saez-Rabanos, and F. J. Aoiz, *J. Phys. Chem A* **109**, 6200 (2005) and references therein.

[6] N. C.-M. Bartlett, D. J. Miller, R. N. Zare, A. J. Alexander, D. Sofikitis, and T. P. Rakitzis, *Phys. Chem. Chem. Phys.* **11**, 142 (2009).

[7] J. C. Juanes-Marcos, S. C. Althorpe, and E. Wrede, *Science* **309**, 1227 (2005).

RAYLEIGH SCATTERING MEASUREMENTS USING CAVITY RING-DOWN SPECTROSCOPY

Doug Kuramoto

Cavity ring-down spectroscopy (CRDS) is an ultrasensitive absorption technique that is capable of measuring absorption changes of 10^{-10} cm^{-1}. In the simplest form of CRDS, two highly reflective mirrors face one another to form an optical cavity. A laser pulse enters the cavity through the back of one mirror and when sufficient intensity has built up, the laser is turned off, deflected, or blocked. The light in the cavity oscillates back and forth, leaking out a small amount of light. The ring down time, or the rate constant of the exponential decay of the light intensity, depends upon all losses of light within the optical cavity. These losses include mirror transmissions, absorption by the chemical sample, and reflection and scattering caused by the sample.

In most CRDS experiments, the absorbance of the sample is determined to measure a trace amount of a species or to resolve a weak absorption peak that is below the detection limit of traditional absorption techniques. We are interested in using CRDS to look at losses caused by the sample other than absorption, more specifically losses caused by Rayleigh scattering. Much of the theory of Rayleigh scattering was developed over 100 years ago. It has been difficult, however, to make direct measurements in the laboratory owing to the small cross section. The extended path length of CRDS makes it possible to measure the total loss caused by atoms or molecules in the gas phase within the cavity. By operating in regions where there are no absorption peaks, the total loss observed is caused primarily by Rayleigh scattering from which the Rayleigh scattering cross section can be determined.

A three mirror CRDS cavity in the ring configuration has recently been built (Figure 1). This configuration adds more complexity to the setup, but it also provides some advantages. One benefit is it results in a small amount of optical feedback to the laser that can used to affect the properties of the laser, which can lead to a more efficient injection of light into the cavity. By measuring the ring down time when the cavity is filled with a sample gas and seeing how the ring down time changes as the contents are replaced with a different sample gas, the magnitude of the Rayleigh scattering cross section can be determined.

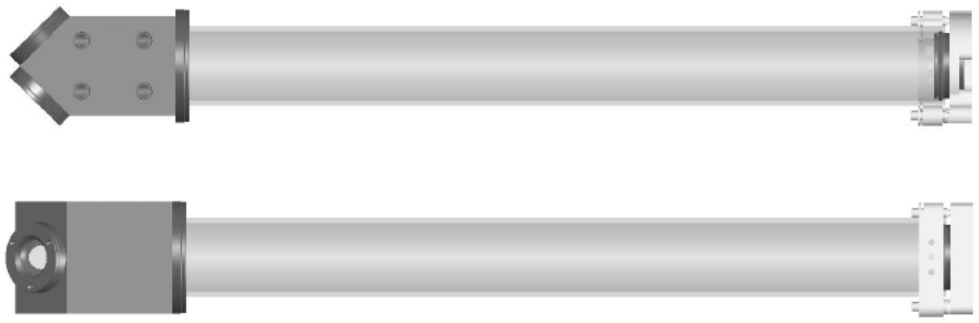

Fig. 1. Three Mirror Cavity Ring-Down Spectroscopy Cavity

MEASUREMENT OF CARBON ISOTOPE RATIOS USING CAVITY RING-DOWN SPECTROSCOPY

Doug Kuramoto

The measurement of isotopes ratios, such as $^{13}C/^{12}C$, is important in chemistry and other fields, such as geology, since it provides useful information on formation and transport processes. The most common method used to measure isotope ratios is the isotope ratio mass spectrometer (IRMS), which is bulky, requires user expertise, and is costly. The measurement of isotope ratios can also be done through absorption spectroscopy using cavity ring-down spectroscopy (CRDS).[1]

We have developed an instrument capable of measuring carbon isotope ratios in organic samples (Figure 1A). The sample is injected into a gas chromatograph (GC) where it is separated into its components. The effluent is passed through a catalytic combustor (C) consisting of platinum and oxidized nickel wires in a ceramic tube heated to 1150 ºC, which completely oxidizes the carbon in the sample to carbon dioxide. The combustion products are fed into a CRDS instrument to measure the concentrations of $^{12}C^{16}O^{16}O$ and $^{13}C^{16}O^{16}O$. We refer to our setup as GC-C-CRDS.

A mixture of methane, ethane, and propane injected in our instrument can be separated, oxidized, and measured as shown in Figure 1B. The chromatographic peaks are used to determine the ratio of $^{13}C/^{12}C$ in the sample. The current instrument can measure isotope ratios with a precision of less than one part per thousand and an accuracy of less than a few parts per thousand. Our instrument does not currently match the capabilities of instruments based on IRMS, but we expect future improvements to make our instrument an attractive alternative to IRMS. Despite the present limitations, the performance is sufficient for certain applications such as those in the oil industry. We plan to test our instrument by measuring isotope ratios of hydrocarbon gasses produced from petroleum sources which can provide useful information during the characterization of an oil reservoir.

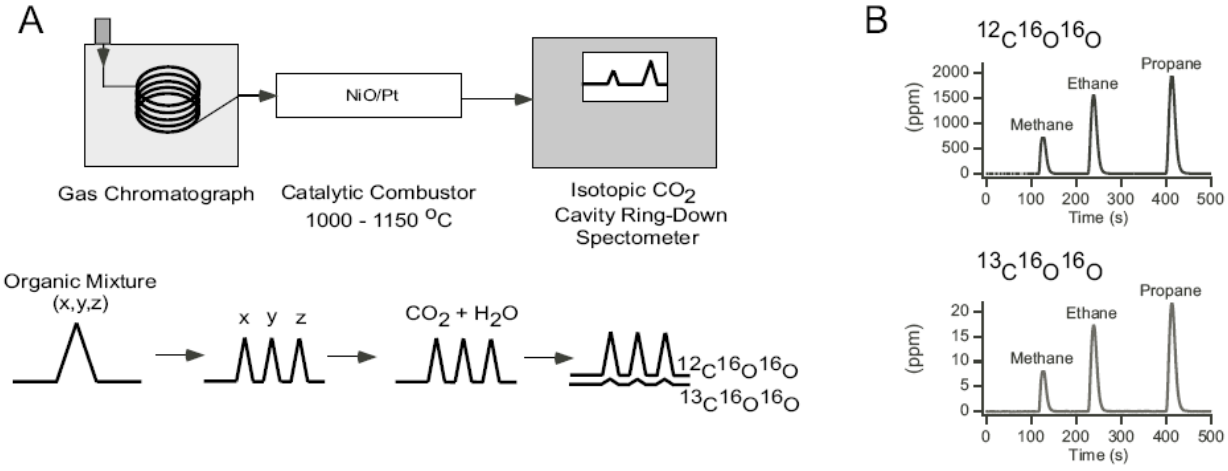

Fig. 1. (A) The GC-C-CRDS instrument. The sample is separated using gas chromatography and combusted to produce carbon dioxide and then the isotopic carbon dioxide concentrations are measured using cavity ring-down spectroscopy. (B) Chromatograms of $^{12}C^{16}O^{16}O$ and $^{13}C^{16}O^{16}O$ produced from a mixture of methane, ethane, and propane.

[1] R. N. Zare, D. S. Kuramoto, C. Haase, S. M. Tan, E. R. Crosson, and N. M. R. Saad, *Proc. Natl. Acad. Sci. (US)* **106**, 10928-10932 (2009).

TWO-STEP LASER MASS SPECTROMETRY OF TERRESTRIAL AND EXTRATERRESTRIAL MATERIALS

Amy Morrow, Hassan Sabbah

Microprobe laser-desorption laser-ionization mass spectrometry (μL^2MS) is a powerful and versatile microanalytical technique that is used to study organic molecules *in situ* in a wide range of terrestrial and extraterrestrial materials. The combination of focused laser-assisted thermal desorption and ultrasensitive laser ionization provides sensitivity, selectivity, and spatial resolution capabilities that are unmatched by traditional methods of analysis. Over the past decade, this laboratory has developed and applied the μL^2MS technique in a number of different research projects. Some areas that we are currently focusing on are:

- **Instrument Development:** To enhance the analytical ability of the μL^2MS technique we are actively pursuing instrument developments. Our plans include: the addition of a camera to visualize desorption and development of the neutral plume; installation of a dye laser to allow adjustment of the ionization laser wavelength; and modification of the sample mounting scheme to allow for more rapid sample analysis.

- **Stability of Organic Compounds Trapped in Aerogel:** This study aims to further our understanding of the potential damaging effects of UV and proton radiation on compounds in both captured particles and innate organic compounds in low-density silica aerogel. Aerogel was a success on the NASA Stardust Mission and may be used for future particle-capture missions as well, making this a timely study.

- **Meteoritics**: Analysis of PAHs in meteorites, meteoritic acid residues and interplanetary dust particles (IDPs). Currently, μL^2MS is being used in investigating the aromatic hydrocarbon contents of the meteorite DaG 476 and fragments of the asteroid 2008TC3, otherwise known as Almahata Sitta.

- **Petroleomics**: Recently, this instrument has been applied to the ongoing controversy over the determination of the correct molecular weight distribution in asphaltenes, a fraction of heavy oil consisting of highly polar and aromatic molecules. Currently, we are testing the ability of this technique to detect relatively high mass (~1500 amu) parent molecules while simultaneously avoiding plasma phase aggregation of low mass parent molecules that would result in a false signal at high m/z.

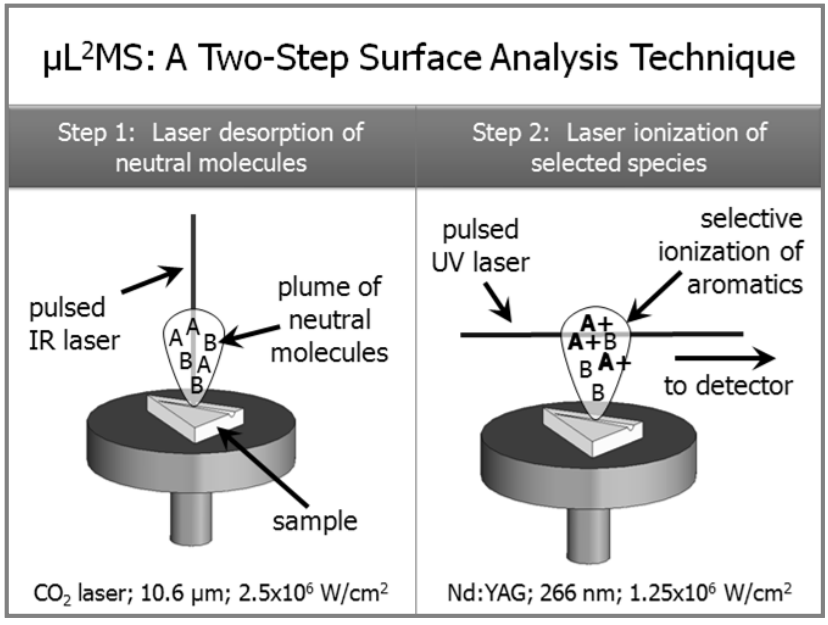

HADAMARD TRANSFORM TIME-OF-FLIGHT MASS SPECTROMETRY

Matthew Robbins, Griffin Barbula, Richard Perry

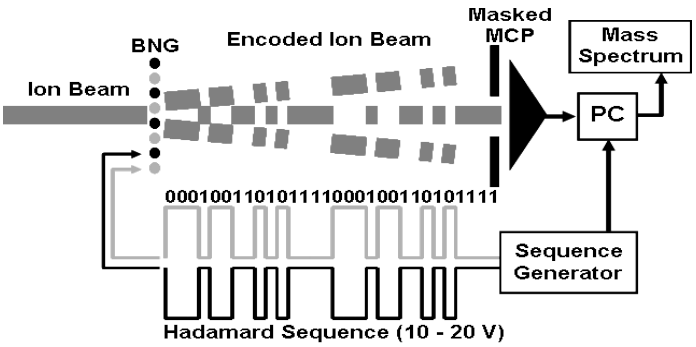

Because time-of-flight mass spectrometry (TOFMS) involves a pulsed detection method, efficient detection of continuous ion sources remains a challenge. Increases in duty cycle (the fraction of ions that are detected) usually come at the expense of mass resolution and/or mass range. In an effort to decouple these figures of merit, our lab has developed a novel form of TOFMS that offers a 100% duty cycle over a wide mass range.[1]

Briefly, in this method ions entering the MS are rapidly switched between two detection states using a known sequence. Because the modulation sequence is based on Hadamard matrices, we have termed this method Hadamard transforms time-of-flight mass spectrometry (HT-TOFMS). Rapid modulation results in multiple ion packets that simultaneously move through the drift region and interpenetrate one another as they fly. In contrast, in a traditional TOFMS experiment a single ion packet moves through the drift region and is detected before a new packet is introduced. In HT-TOFMS, the acquired signal is the time-shifted superposition of all the packets' mass spectra which can be decoded using knowledge of the applied modulation sequence. Because the modulation scheme allows us to detect more ions per unit time when compared to traditional, on-axis TOFMS, HT-TOF produces mass spectra with increased signal-to-noise properties, permits greater detection sensitivity, or enables faster spectral acquisition. Some areas of active research are:

- **New Ion Gating Devices and Ion Optics:** In HT-TOFMS, Bradbury-Nielson gates are used for modulation of the ion beam. We continue to develop techniques for macro-[4] and microfabrication[5] of these devices and test their applicability for our method.
- **Imaging TOF:** Because 100% duty cycle work requires a two anode detector, we have worked to expand our research using arbitrary position detection systems. We currently employ multichannel plate detectors with delay line anodes in acquisition of our HT-TOF data.
- **HT-TOFMS Kinetics:** Because HT-TOF is a 50 or 100% duty cycle technique, more ions are collected within a given time window than with traditional TOFMS. This signal advantage can in turn be used to acquire more statistically significant spectra in a given time period. HT-TOFMS has the potential to push into the millisecond regime of kinetics where other modern MS is limited to seconds in full scan mode.
- **Coupling to Chromatographic and Electrophoretic Separations**: The continuous nature and high spectral acquisition rate of HT-TOFMS make it an ideal detector for separation techniques, particularly those which produce time-narrow peaks.
- **DESI:** Desorption electrospray ionization (DESI), an ambient pressure ionization technique, has shown promise for high sample throughput. By coupling DESI to HT-TOFMS, the sampling rate of DESI can be tested in a regime not accessible by other MS techniques with lower spectral acquisition rates.

[1] O. Trapp, J. R. Kimmel, O. K. Yoon, I. A. Zuleta, F. M. Fernandez, and R. N. Zare, "Continuous Two-Channel Time-of-Flight Mass Spectrometric Detection of Electrosprayed Ions," *Angew. Chem. Int. Ed.* **43**, 6541-6544 (2004).

[2] J. R. Kimmel, O. K. Yoon, I. A. Zuleta, O. Trapp, and R. N. Zare, "Peak Height Precision in Hadamard Transform Time-of-Flight Mass Spectra," *J. Am. Soc. Mass Spectrom.* **16**, 1117-1130 (2005).

[3] O. K. Yoon, I. A. Zuleta, M. D. Robbins, and R. N. Zare, "Duty Cycle and Modulation Efficiency of Two-Channel Hadamard Transform Time-of-Flight Mass Spectrometry," *J. Am. Soc. Mass Spectrom.* **16**, 1888-1901 (2005).

[4] O. K. Yoon, I. A. Zuleta, M. D. Robbins, G. K. Barbula, and R. N. Zare, "Simple Template-Based Method to Produce Bradbury-Nielsen Gates," *J. Am. Soc. Mass Spectrom.* **18**, 1901-1908 (2007).

[5] I. A. Zuleta, G. K. Barbula, M. D. Robbins, O. K. Yoon, and R. N. Zare, "Micromachined Bradbury-Nielsen Gates," *Anal. Chem.* **79**, 9160-9165 (2007).

[6] M. D. Robbins, O. K. Yoon, I. A. Zuleta, G. K. Barbula, and R. N. Zare, "Computer-Controlled, Variable-Frequency Power Supply for Driving Multipole Ion Guides," *Rev. Sci. Inst.* **79**, 034702 (2008).

[7] O. K. Yoon, M. D. Robbins, I. A. Zuleta, G. K. Barbula, and R. N. Zare, "Continuous Time-of-Flight Ion Imaging: Application to Fragmentation," *Anal. Chem.* **80**, 8299 (2008).

PHOSPHOPEPTIDE PROFILE FOR THE EARLY DIAGNOSIS OF MINIMAL RESIDUAL DISEASE IN RESPONSE TO DOXORUBICIN TREATMENT OF LEUKEMIA

Songyun Xu, John C. Whitin, Harvey J. Cohen

Leukemia relapse occurs in at least 20% of children with acute lymphoblastic leukemia treated with chemotherapy drugs. This observation leads to the hypothesis that the proteomes of these two groups, distinguished by the occurrence of relapse, differ in their specific protein expression patterns and protein post-translational modifications. Protein-based biomarkers from minimal residual disease following treatment of acute lymphoblastic leukemia using chemotherapy drugs have great potential as new diagnostic tool. The levels of up- and down-modification of peptides and proteins resulting from diseased cell may signal various clinical features and diagnostic clues. We present a method that uses zirconium phosphate beads to purify phosphopeptides and phosphoprotein, followed with SELDI mass spectrometry to study phosphoproteomic patterns.

The cell growth process in response to treatment with the chemotherapy drug doxorubicin was assessed with a hemacytometer over a three day period. The result is shown in Figure 1. When REH human leukemia cells were treated with 8 μL of 290 nM doxorubicin, the cell concentration in the media was nearly constant at 0.5 million cells per milliliter. For the control sample which was not treated with doxorubicin, the cell concentration tripled in the same time period.

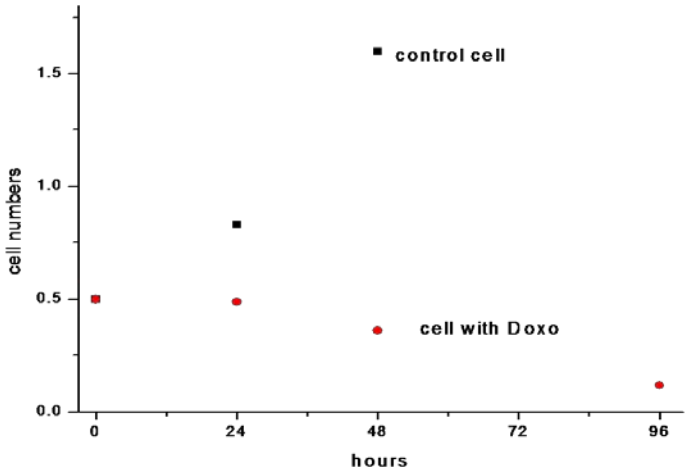

Fig. 1. Cell growth process in response to treatment with (red dot) and without (black dot) the chemotherapy drug doxorubicin

The phosphopeptide profile of the leukemia cell extract following treatment was analyzed daily for three days using SELDI MS and compared to the untreated extract. We detected 15 major peaks in the mass spectrum from the isolated phosphopeptides from the doxorubicin treated cells that monotonically decreased: m/z 1916, 2115, 2126, 2165, 2193, 2214, 2242, 2320, 2516, 2723, 3558, 3481, 4290, 4410, and 4610. We also detected 3 peaks in the mass spectrum from the isolated phosphopeptides specific to the doxorubicin treated cells that monotonically increased: m/z 4580, 6210, and 6290. These 18 peaks comprise a phosphopeptide profile for the early diagnosis of minimal residual disease in response to doxorubicin treatment of leukemia cell disease.

PHOTOPOLYMERIZED SOL-GEL AS CHROMATOGRAPHIC MEDIA AND CHEMICAL REACTORS

Maria T. Dulay

Our work focuses on the use of porous photopolymerized sol-gel (PSG) materials to create chromatographic media for separations as well as on-line chemical reactors. We developed a synthetic method based on sol-gel chemistry (hydrolysis and condensation reactions) and photochemistry for the preparation of a photopolymerized sol-gel (PSG) monolith. The methacrylate group of a trialkoxysilane reagent is photoactivated to produce PSG in a 5-min reaction. The light source can be UV or visible. Our sol-gel technique includes template-based processing where the silicate matrix is assembled around a suitable template or porogen to form cavities of a specific size and shape within the cross-linked host. With the presence of free silanol groups on the PSG monolith a variety of different functional groups can be covalently grafted to the monolith surface, allowing us to tailor the selectivity of the monolith.

We have had considerable success in recent years with the use of PSG materials for separation and preconcentration of dilute mixtures of analytes. The on-line preconcentration feature of our macroporous PSG monolith offers an alternative to existing sample enrichment schemes. While the typical injected sample volume ranges from 1 nL to 30 nL, the PSG monolith allows for injection volumes up to 10 μL because of high mass transfer and high convective flow in the monolith structure, allowing up to 1000-fold preconcentration of dilute test samples. We are currently working on creating a protein and peptide concentrator on-line with capillary electrophoresis.

The PSG monolith can be thought of as a building block for the preparation of different on-column chemical devices, including enzyme microreactors for extraction of sugar precursors in the biofuel preparation process, affinity materials through entrapment of zirconium nanoparticles for phosphopeptide binding, and catalytic reactors for organic transformations. These devices are formed in a capillary column downstream from separation techniques such as capillary electrophoresis and capillary electrochromatography. We have demonstrated the use of trypsin-immobilized PSG materials for on-line enzymatic digestions with 2000 times enhancement in the digestion rate of an artificial substrate as compared to the bulk solution rate. Our success with trypsin-PSG materials for capillary columns is the basis for our current work that involves the creation of enzyme microreactors.

More generally, we want to expand the use of the PSG material for on-line organic reactions. The PSG monolith can be used to entrap catalytic materials or the monolith can be used as a support matrix for chemicals that can effect a chemical reaction. For example, a PSG material with covalently bound amine groups has the potential to be used in Knoevenagel condensation reactions at room temperature with downstream chromatographic or electrophoretic separation of the products. A PSG chemical reactor will allow us to combine synthesis, separation, and detection of products in one step in our capillary system. The advantages of such a device include small volumes of reagents and starting materials and an increase in the number of different reactions that can be run. In addition, there is some evidence to suggest that immobilization of a catalyst can lead to improvements in the efficiency and activity of the catalyst.

MICROFLUIDIC DEVICE COUPLED WITH SURFACE PLASMON RESONANCE IMAGING

Logan Leslie

In the field of biological science, heterogeneous-phase biochemical assays, including both immunoassays and nucleic acid hybridization assays, have been among the most powerful analytical techniques. Traditionally, the assays in this type, such as the enzyme-linked immunosorbent assay (ELISA) are carried out without sample replenishment in containers having milliliter scale volumes. Having such high sample consumption for rare samples presents a limitation. Moreover, ELISA relies on an enzyme-conjugated secondary antibody to couple with the immunocomplex for generating signals for measurement. Until the end of an ELISA, no information can be obtained from the assay. When analyzing samples in low quantity, ELISA often takes hours to complete.

To develop a system for running heterogeneous-phase biological assays with higher rapidity and lower sample consumption, we combine a microfluidic device, made of polydimethylsiloxane (PDMS) and an array of thin gold spots, with surface plasmon resonance (SPR) imaging. The combined system offers significant advantages: (1) the microfluidic device provides flow channels with nanoliter volumes, by which the heterogeneous-phase reactions are accelerated because the reagents are quickly replenished by the liquid flow; (2) the use of microfluidics allows an immunoassay to be carried out with less sample consumption; and (3) SPR imaging gives real-time monitoring of the formation of an immunocomplex or a hybridized complex by sensing the refractive index change of binding molecules to the surfaces of gold spots giving kinetic data on the process. Moreover, signal amplification is available for SPR imaging by applying an additional gold-nanoparticle-linked reagent. The results below show the excellent performance of the combined system and indicate the potential clinical applications.

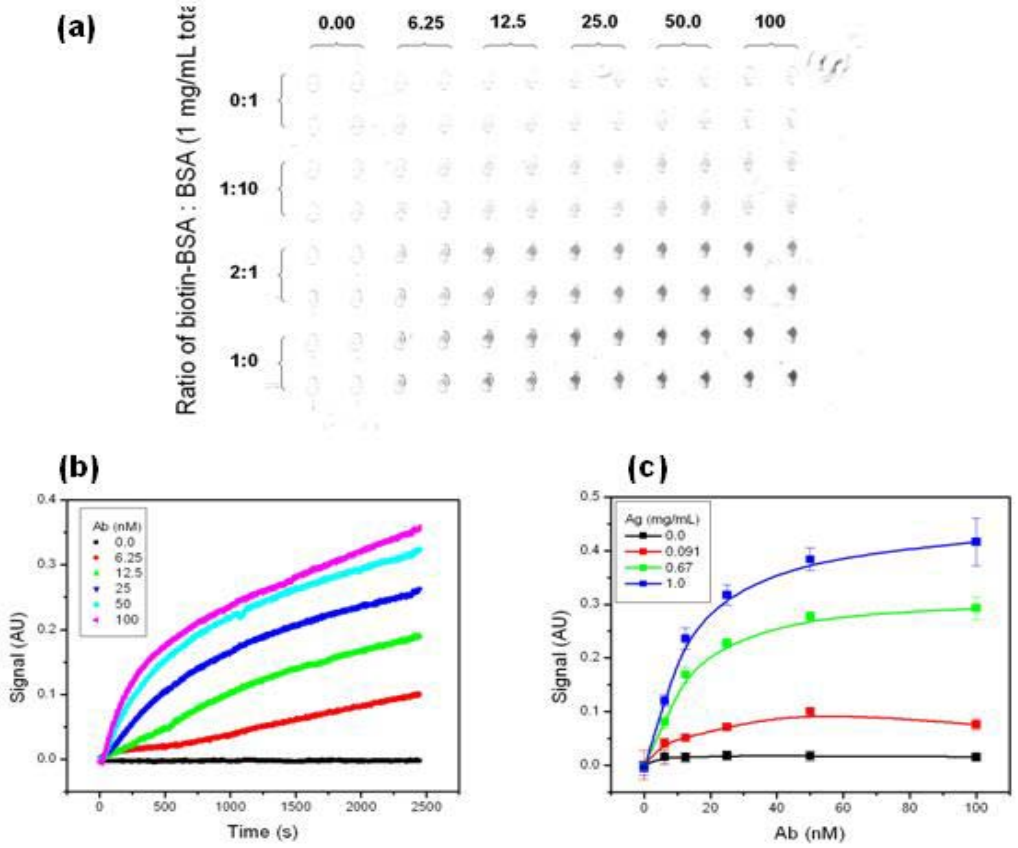

Fig. 2. (a) Background corrected end-point SPR image of the microfluidic chip obtained after anti-biotin antibody binding to biotinylated BSA covered gold spots. (b) Kinetic curves of anti-biotin antibody binding to pure biotinylated BSA covered gold spots. (c) End-point calibration curves of the density of bound anti-biotin antibody versus its working concentration.

SINGLE-CELL ANALYSIS ON A MICROFLUIDIC PLATFORM

Eric Hall, Peng Guo, Bor-han Chueh

In the study of a biological population, how important is individuality? Are the members of the population so similar that the average behavior can describe them all, or are deviations significant enough to make this kind of description misleading? The conventional techniques in biology use a large number of cells and generate the ensemble averaged values to describe cellular characteristics. These methods are fast and efficient ways of observation as long as the individual cells exhibit little deviation from this *average* behavior. However, if the deviations *are* significant, the large-scale ensemble averaging methods fail to give a proper picture of biological phenomena. A simple example will be the case of a bimodal distribution, where the cells with an average behavior actually represent a smaller fraction of the population.

Recent advances in microfluidics opened up a new possibility in single-cell biology by providing the necessary toolkits for handling and analyzing individual cells. We believe that it is an opportune time to apply microfluidic technologies to investigate individuality of cells because important information relevant to the most pressing biological questions is very likely obfuscated by ensemble averaging techniques. Our section develops techniques for performing single-cell analysis on a microfluidic device, more commonly referred to as "lab-on-a-chip". We have made pioneering contributions to the field, including the development of a device capable of capturing a single cell and delivering precise amounts of reagents,[1] and an on-chip chemical cytometer integrated with a picoliter micropipette for cell lysis and derivatization.[2] More recently, we have extended this technology to study the phycobilisome degradation process in individual cyanobacteria cells.[3]

There are currently two main goals in our section. The first is to develop a microfluidic device capable of capturing a large number of single cells and sustaining them in an on-chip culture for a prolonged period of time, using two layers of channels separated by a membrane of conical nanopores (**Fig. 1**). This will allow for time-resolved observation of a statistically significant number of single cells, an ability currently lacking in flow cytometry and traditional microscopy-based approach. The second goal is to integrate this design with an on-chip device capable of extracting and amplifying sufficient DNA from a single cell for sequencing **(Fig. 2)**.

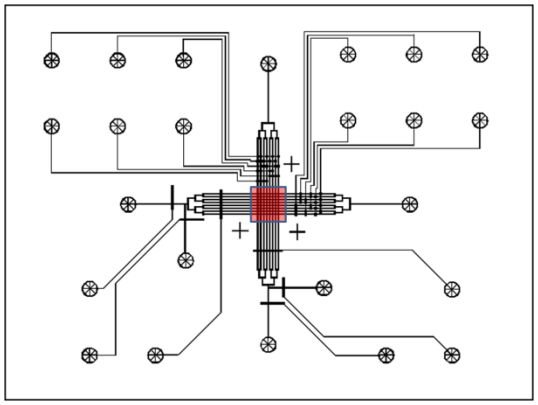

Fig. 1. Microfluidic channels and control valves (black) facilitate the capture of single cells on a nanoporous membrane (red).

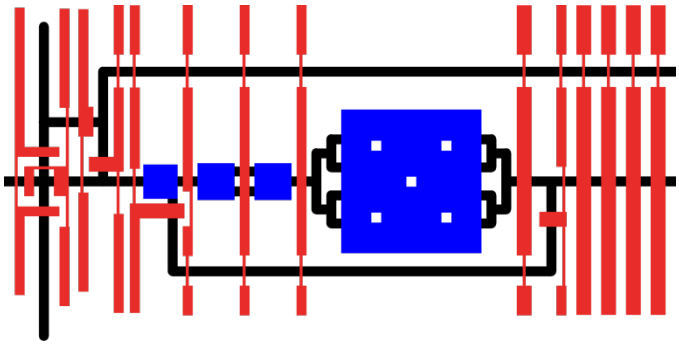

Fig. 2. Cells are manipulated with microfluidic channels (black) and control valves (red) into chambers (blue) designed to deliver specific nanoliter volumes of reagents.

[1] A.R. Wheeler, W.R. Throndset, R.J. Whelan, A.M. Leach, R.N. Zare, Y.H. Liao, K. Farrell, I.D. Manger, and A. Daridon, *Anal. Chem.* **75**, 3581 (2003).
[2] H. Wu, A.R. Wheeler, and R.N. Zare, *Proc. Natl. Acad. Sci. U.S.A.* **101**, 12809 (2004).
[3] B. Huang, H. Wu, D. Bhaya, A.R. Grossman, S. Granier, B.K. Kobilka, and R.N. Zare, *Science* **315**, 81 (2007).

DEVELOPMENT OF A CELL SORTER BASED ON INTEGRATION OF POROUS MEMBRANES INTO LAYERED MICROFLUIDIC DEVICES

Bor-han Chueh, Cheuk-wing Li, and Huiling Wu

Layered microfluidic devices integrated with porous polycarbonate or polyester membranes have been widely used for mass transport control, immunoassays, and blood cell sorting. The placement of a semi-porous membrane at the interface of two channel layers is crucial to minimize unwanted crossover of fluid flows between microchannels while allowing diffusive mixing of reagents. Several methods have been reported to seal off the crevices inevitably generated because of the thickness of the membrane. For example, the application of PDMS pre-polymer as a mortar layer could prevent the leakage along the membrane. This method provides robust and reliable bonding between two PDMS layers. However, in the case of thicker membranes and/or narrower channels, the mortar layer method can clog the channels easily.

We introduce an alternative strategy of directly using PDMS as a porous membrane itself to fabricate monolithic microfluidic devices. In this case, the integration of a porous PDMS membrane can be completed without clogging microchannels by plasma oxidation or by utilizing different mixing ratios for curing PDMS polymers. To prepare porous PDMS membranes, SU-8 posts with different sizes are created on a silicon wafer. A thin film of PDMS is prepared by spin coating the wafer. The resulting thin PDMS with holes is lifted cleanly off the wafer using a specially designed cured PDMS frame. This method allows varying sizes of pores on a single membrane, compared to commercially available porous membranes with a fixed pore size. We demonstrate the use of this method to fabricate a particle sorter where different sizes of microbeads can be filtered through different sizes of pores of the membranes.

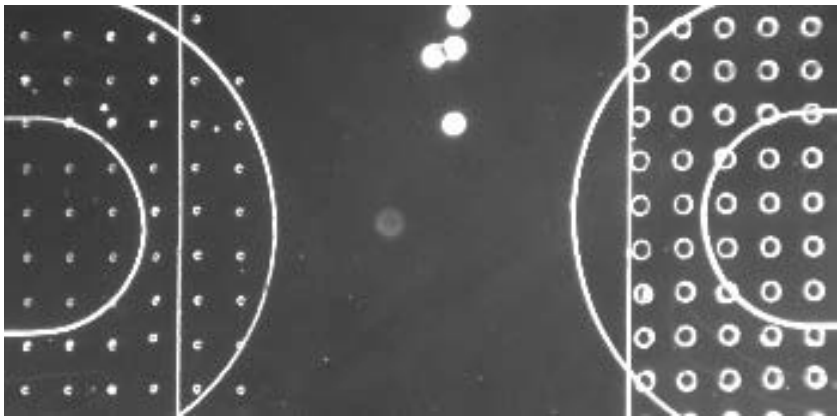

Two different sizes of pores (10 and 35 μm) in a PDMS membrane embedded into a microfluidic device

NANOPARTICLE FORMATION USING SUPERCRITICAL FLUID TECHNOLOGY

Gunilla B. Jacobson, Tatsiana Lobovkina, Yaping Zhao

We have specific interest in preparing nanoparticles of therapeutic compounds whose size and surroundings can be controlled. Important pharmaceutical issues, such as chemical and physical stability, dissolution rate, and therapeutic performance, are often related to particle size, morphology, and surface properties. By working on the nanoscale range new drug delivery systems can be explored, as well as increased target specificity along with lower dosage requirements and therefore lower unwanted side effects.

We are using supercritical carbon dioxide as an antisolvent in the preparation of our particles. When a fluid is taken above its critical temperature (Tc) and critical pressure (Pc), it exists in a condition called a supercritical fluid (SCF), Figure 1. It is the possibility of controlling the solvent properties of a SCF by small changes in temperature and pressure that make SCFs unique for the desired tight process control. Also, the high diffusivity of SCFs allows much faster diffusion into the liquid solvent and formation of supersaturation of the solute. This in turn allows for much smaller nanosized particles to be formed as well as control of the size distribution, as compared to using liquid antisolvents, or other techniques such as jet milling.

In addition, we are exploring the encapsulation of the nanoparticles by various means for the purpose of increasing their stability or their targeting or both. Encapsulation will also enable designed characteristics for distribution and release of the active compounds within the nanoparticles. The work ranges from fundamental studies of how nanoparticles are formed in supercritical fluids to how they can be used in pharmaceutical applications by studying their use in sustained release experiments and distribution in living organisms.

As an example, luciferin nanoparticles dispersed in the biodegradable polymer poly(lactic acid) (PLA) have been formed and tested both *in vitro* and *in vivo*. Bioluminescence imaging of transgenic mice that have been genetically engineered to universally express luciferase, shows a slow and sustained release of luciferin over 20 days upon subcutaneous injection of these particles (Figure 2). Using luciferin as a model drug we can explore the effect of particle size and composition on its distribution *in vivo*. This knowledge is then transferred to other therapeutics to optimize the particles for each specific drug.

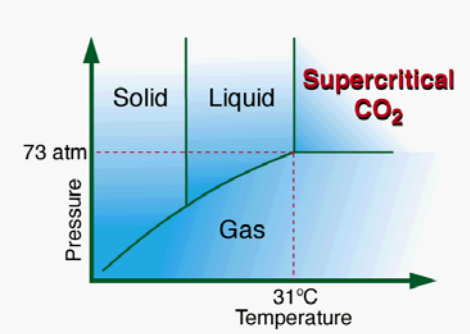

Figure 1. Phase diagram of carbon dioxide.

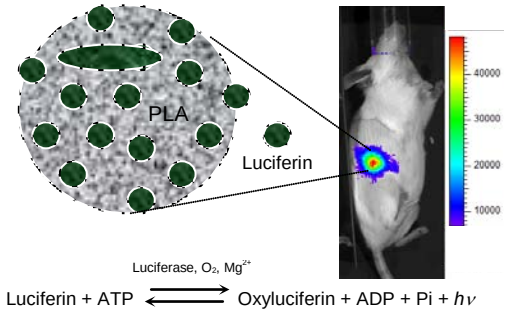

Figure 2. Bioluminescence image of luciferin/PLA particles 20 days post injection.

SOME SELECTED RECENT PUBLICATIONS

FUNDAMENTAL REACTION DYNAMICS STUDIES

N. T. Goldberg, J. Zhang, K. Koszinowski, F. Bouakline, S. C. Althorpe, and R. N. Zare, "Vibrationally Inelastic H + D_2 Collisions Are Forward Scattered," *Proc. Natl. Acad. Sci. USA* **105**, 18194-18199 (2008).

N. C. M. Bartlett, D. J. Miller, A. J. Alexander, D. Sofikitis, T. P. Rakitzis, and R. N. Zare, "Time-Dependent Depolarization of Aligned HD Molecules," *Phys. Chem. Chem. Phys.* **11**, 142-147 (2008).

S. J. Greaves, E. Wrede, N. T. Goldberg, J. Zhang, D. J. Miller, and R. N. Zare, "Vibrational Excitation Through Tug-of-War Inelastic Collisions," *Nature* **454**, 88-91 (2008).

J. A. Beswick and R. N. Zare, "On the Quantum and Quasiclassical Angular Distributions of Photofragments," *J. Chem. Phys.* **129**, 164315-1-9 (2008).

K. Koszinowski, N. T. Goldberg, J. Zhang, R. N. Zare, F. Bouakline, and S. C. Althorpe, "Differential cross section for the H + $D_2 \rightarrow$ HD (v' = 1, j' = 2, 6, 10) + D reaction as a function of collision energy," *J. Chem. Phys.* **127**, 124315 (2007).

N. T. Goldberg, K. Koszinowski, A. E. Pomerantz, and R. N. Zare, "Doppler-free ion imaging of hydrogen molecules produced in bimolecular reactions," *Chem. Phys. Lett.* **433**, 439-443 (2007).

M. R. Martin, D. J. A. Brown, A. S. Chiou, and R. N. Zare, "Reaction of Cl with CD_4 excited to the second C-D stretching overtone," *J. Chem. Phys.* **126**, 44315-44316 (2007).

J. P. Camden, H. A. Bechtel, D. J. A. Brown, and R. N. Zare, "Comparing reactions of H and Cl with C-H stretch-excited CHD_3," *J. Chem. Phys.* **124**, 1-7 (2006).

ABSORPTION SPECTROSCOPY

Thermal Lensing

F. Yu, A. A. Kachanov, A. Wainright, and R. N. Zare, "Ultraviolet Thermal Lensing Detection of Amino Acids," *J. Chromatography A* **1216**, 3423-3430 (2009).

Cavity Ring-down Spectroscopy

R. N. Zare, D. S. Kuramoto, C. Haase, S. M. Tan, E. R. Crosson, and N. M. R. Saad, "High-Precision Optical Measurements of $^{13}C/^{12}C$ Isotope Ratios in Organic Compounds at Natural Abundance," *Proc. Natl. Acad. Sci. (US)* **106**, 10928-10932 (2009).

MASS SPECTROMETRY

Two-Step Laser Mass Spectrometry of Terrestrial and Extraterrestrial Materials

A. Pomerantz, M. Hammond, A. Morrow, and R. N. Zare, "Asphaltene Molecular Mass Distribution Determined by Two-Step Laser Mass Spectrometry," *Energy & Fuels* **23**, 1162-1168 (2009).

A. E. Pomerantz, M. R. Hammond, A. L. Morrow, O. C. Mullins, and R. N. Zare, "Two-Step Laser Mass Spectrometry of Asphaltenes," *J. Am. Chem. Soc.* **130**, 7216-7217 (2008).

M. K. Spencer, S. J. Clemett, S. A. Sandford, D. S. McKay, and R. N. Zare, "Organic Compound Alteration during Hypervelocity Collection of Carbonaceous Materials in Aerogel," *Meteoritics and Planetary Science* **44**, 15-24 (2009).

J. E. Elsila, N. P. De Leon, P. R. Buseck, and R. N. Zare, "Alkylation of polycyclic aromatic hydrocarbons in carbonaceous chondrites," *Geochimica et Cosmochimica Acta,* **69**, 1349 (2005).

Hadamard Transform Time-of-Flight Mass Spectrometry

O. K. Yoon, M. Robbins, I. Zuleta, G. Barbula, and R. N. Zare, "Continuous Time-of-Flight Ion Imaging: Application to Fragmentation," *Anal. Chem.* **80**, 8299-8306 (2008).

O. K. Yoon, I. A. Zuleta, M. D. Robbins, G. K. Barbula, and R. N. Zare, "Simple template-based method to produce Bradbury-Nielsen Gates," *J. Am. Soc. Mass Spectrom.*, in press (2007).

O. K. Yoon, I. A. Zuleta, J. R. Kimmel, M. D. Robbins, and R. N. Zare, "Duty cycle and modulation efficiency of two-channel Hadamard Transform time-of-flight mass spectrometry," *J. Am. Soc. Mass Spectrom.* **16**, 1888-1901(2005).

J. R. Kimmel, O. K. Yoon, I. A. Zuleta, O. Trapp, and R. N. Zare, "Peak height precision in Hadamard Transform time-of-flight mass spectra," *J. Am. Soc. Mass Spectrom.* **16**, 1117-1130, (2005).

CAPILLARY ELECTROPHORESIS

N. Johannesson, E. Pearce, M. T. Dulay, R. N. Zare, J. Berquist, and K. E. Markides, "On-line biological sample cleanup for electrospray mass spectrometry using sol-gel columns," *J. Chromatogr. B* **842**, 70-74 (2006).

M. T. Dulay, Q. J. Baca, and R. N. Zare, "Enhanced proteolytic activity of covalently bonded enzymes in photopolymerized sol-gel," *Anal. Chem.* **77**, 4604-4610 (2005).

SURFACE-PLASMON RESONANCE IMAGING

Y. Luo, F. Yu, and R. N. Zare, "Microfluidic Device for Immunoassays Based on Surface Plasmon Resonance Imaging," *Lab Chip* **8**, 694-700 (2008).

B. Huang, F. Yu, and R. N. Zare, "Surface plasmon resonance imaging using a high numerical aperture microscope objective," *Anal. Chem.* **79**, 2979-2983 (2007).

MICROFLUIDICS AND SINGLE-MOLECULE SPECTROSCOPY

Y. Luo and R. N. Zare, "Perforated Membrane Method for Fabricating Three-Dimensional Polydimethylsiloxane Microfluidic Devices," *Lab on a Chip* **8**, 1688-1694 (2008).

T. D. Perroud, M. P. Bokoch, and R. N. Zare, "Cytochrome *c* conformations resolved by the photon-counting histogram: watching the alkaline transition with single-molecule sensitivity," *Proc. Natl. Acad. Sci. U.S.A.* **102**, 17570 (2005).

S. Granier, S. Kim, A. M. Shafer, V. R. P. Ratnala, J. J. Fung, R. N. Zare, and B. K. Kobilka, "Structure and conformational changes in the C-terminal domain of the beta 2-adrenoceptor: insights from fluorescence resonance energy transfer studies," *J. Biol. Chem.* **282**, 13895 (2007).

B. Huang, H. Wu, D. Bhaya, A. R. Grossman, S. Granier, B. K. Kobilka, and R. N. Zare, "Counting low-copy-number proteins in a single cell," *Science* **315** (2007).

H. K. Wu, B. Huang, and R. N. Zare, "Generation of complex, static solution gradients in microfluidic channels," *J. Am. Chem. Soc.* **128**, 4194-4195 (2006).

B. Huang, H. K. Wu, S. Kim, B. K. Kobilka, and R. N. Zare, "Phospholipid biotinylation of polydimethylsiloxane (PDMS) for protein immobilization," *Lab on a Chip* **6**, 369-373 (2006).

NANOPARTICLE SYNTHESIS, CHARACTERIZATION AND APPLICATION

G. B. J. Andrews, R. Shinde, C. H. Contag, and R. N. Zare, "Drugs Dispersed in Polymer Nanoparticles for Sustained Release," *Angew. Chem. Int. Ed.* **47**, 7880-7882 (2008).

ZARELAB CONTACT LIST

Lab Member		Office Phone[1]	Office/Lab[2]	**EMAIL**
Griffin	**BARBULA**	723-4332	M 017B	barbula@stanford.edu
Nate	**BARTLETT**	723-4333	M 017A	nbartlet@stanford.edu
Bor-han	**CHUEH**	723-8280	C E250	chueh@stanford.edu
Maria	**DULAY**	723-8280	C E250	mdulay@stanford.edu
Peng	**GUO**	723-8280	C E250	dd0351@stanford.edu
Eric	**HALL**	723-8280	M E250	erichall@stanford.edu
Gunilla	**JACOBSON**	725-0690	C E250	gunilla@stanford.edu
Justin	**JANKUNAS**	725-2983	M 315	jankunas@stanford.edu
Doug	**KURAMOTO**	723-4333	M O17A	kuramoto@stanford.edu
Dave	**LEAHY**	723-4393	M 131	djleahy@stanford.edu
Logan	**LESLIE**	723-8280	C E250	lleslie@stanford.edu
Wing	**LI**	723-8280	C E250	wingli@stanford.edu
Tanya	**LOBOVKINA**	723-8280	C E250	tatsiana@stanford.edu
Barbara	**MARCH**	723-4313	M 133	march1@stanford.edu
Amy	**MORROW**	723-4318	M 317	almorrow@stanford.edu
Matt	**ROBBINS**	723-4398	M 017B	mdr@stanford.edu
Hassan	**SABBAH**	723-4318	M 317	sabbah@stanford.edu
Huiling	**WU**	723-8280	C E250	huilingw@stanford.edu
Songyun	**XU**	723-4334	M 017C	syxu@stanford.edu
Dick	**ZARE**	723-3062	M 133	zare@stanford.edu
Jianyang	**ZHANG**	725-2983	M 315B	jyzhang6@stanford.edu
Yaping	**ZHAO**	723-8280	C E250	ypzhao@stanford.edu

[1] Area Code: 650

[2] M = S. G. Mudd building; C = J. H. Clark Center

THE ZARELAB


Richard Zare


Griffin Barbula


Nate Bartlett

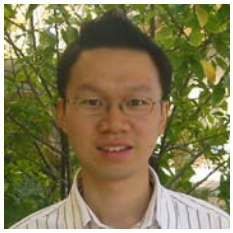
Bor-han Chueh


Maria Dulay


Peng Guo


Eric Hall


Gunilla Jacobson


Justin Jankunas


Doug Kuramoto


David Leahy


Logan Leslie


Tanya Lobovkina


Barbara March


Amy Morrow


Matt Robbins


Hassan Sabbah


Huiling Wu


Songyun Xu


Yaping Zhao

FLOOR PLAN OF LABS AND OFFICES – S.G. MUDD BLDG. BASEMENT

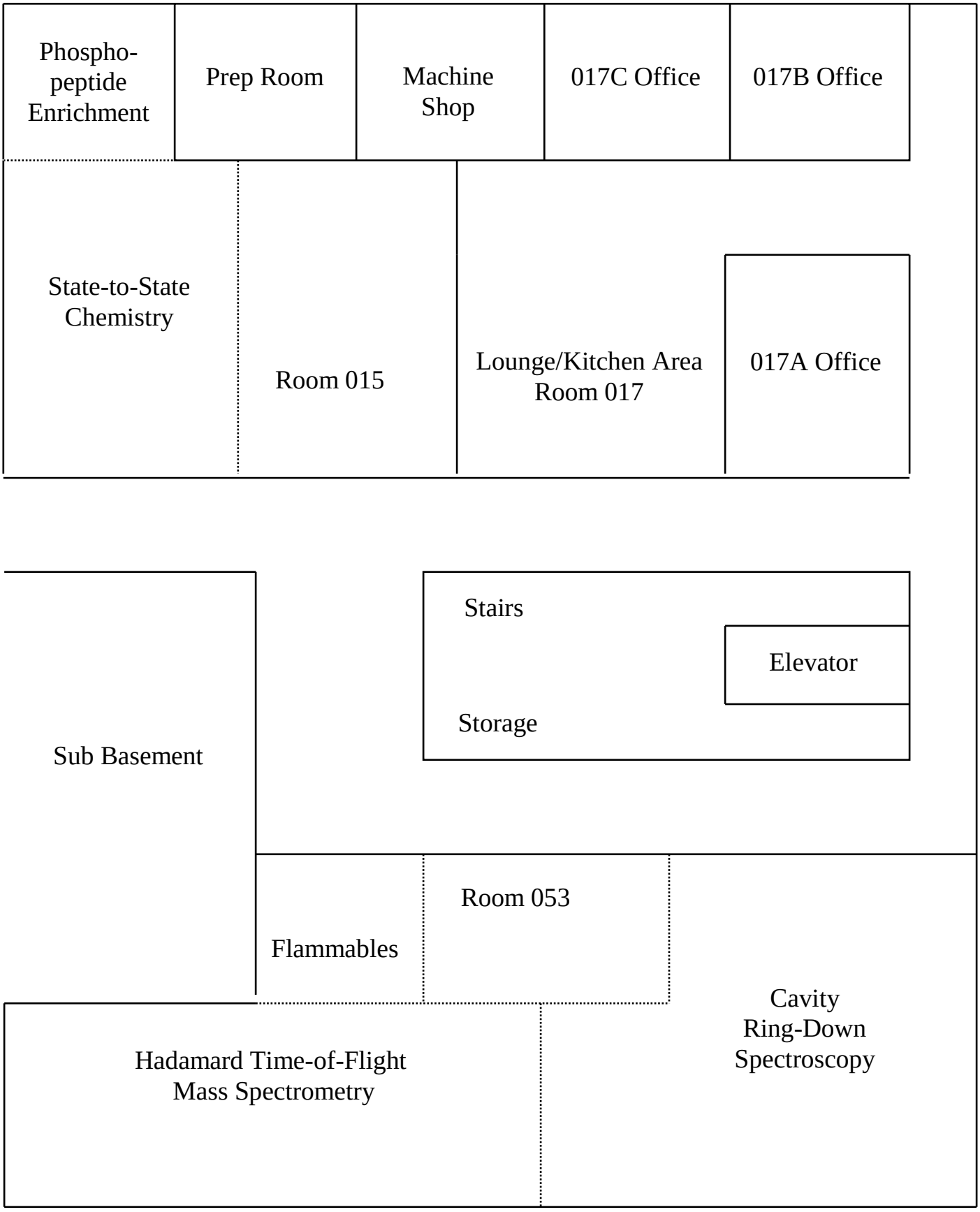

FLOOR PLANS OF LABS AND OFFICES – S.G. MUDD BLDG. 1st and 3rd FLOOR

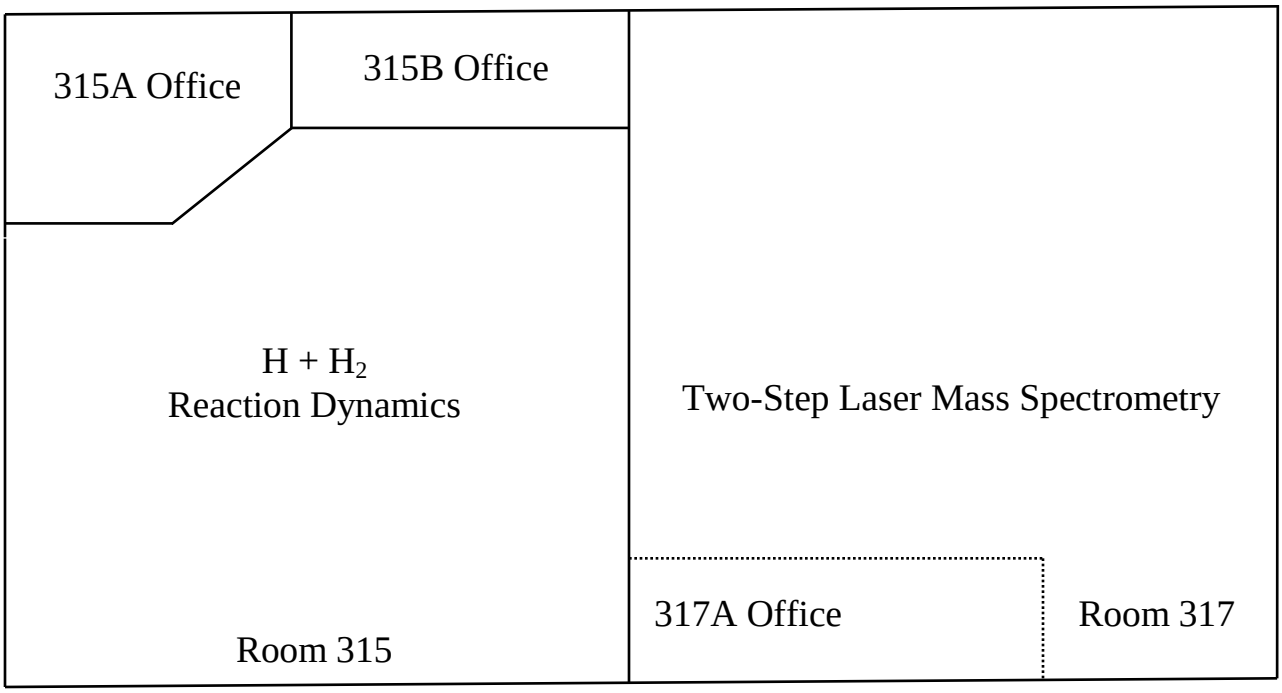

MUDD, 3rd FLOOR

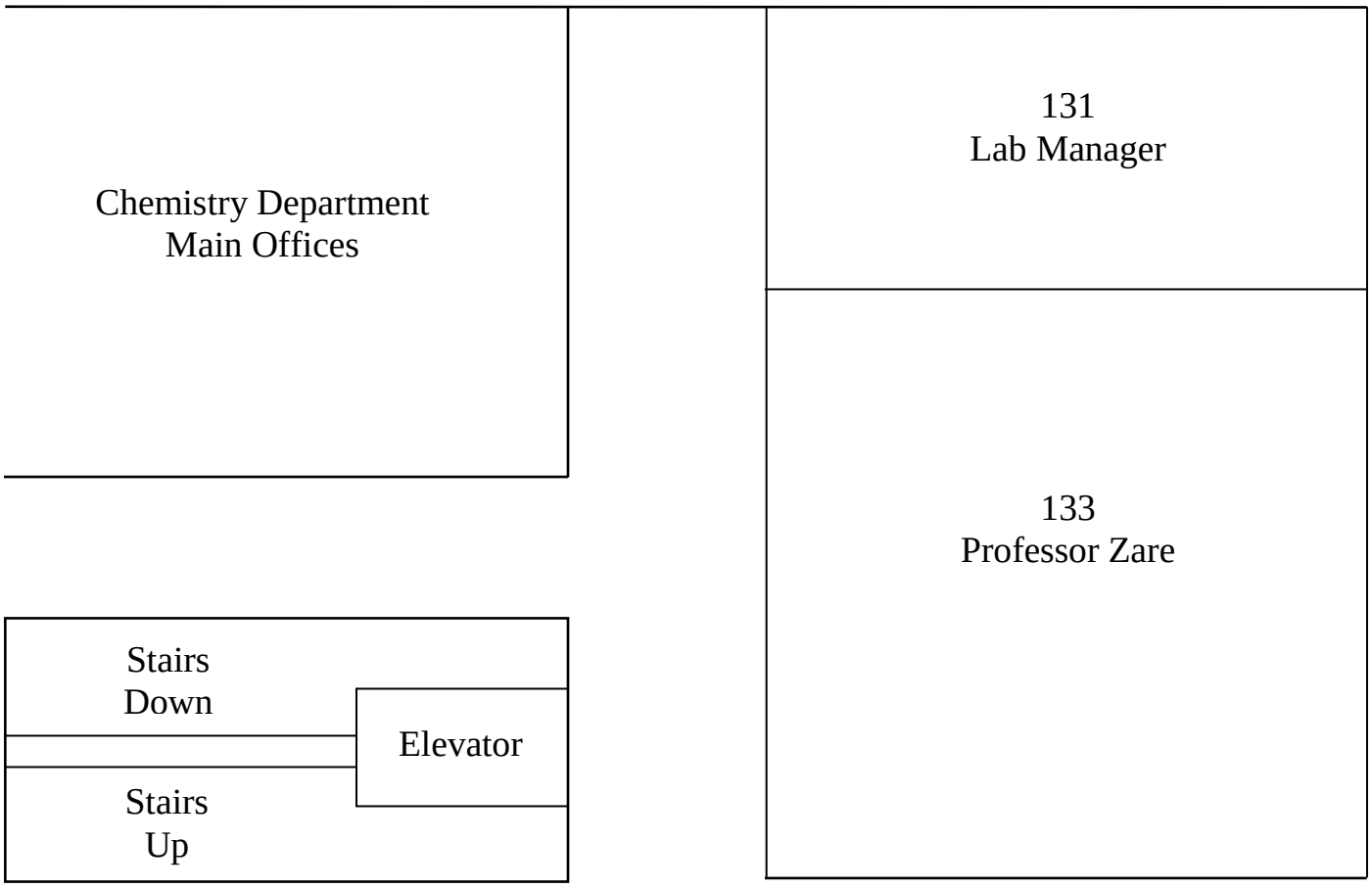

MUDD, 1ST FLOOR

FLOOR PLAN OF LABS – J.H. CLARK CENTER

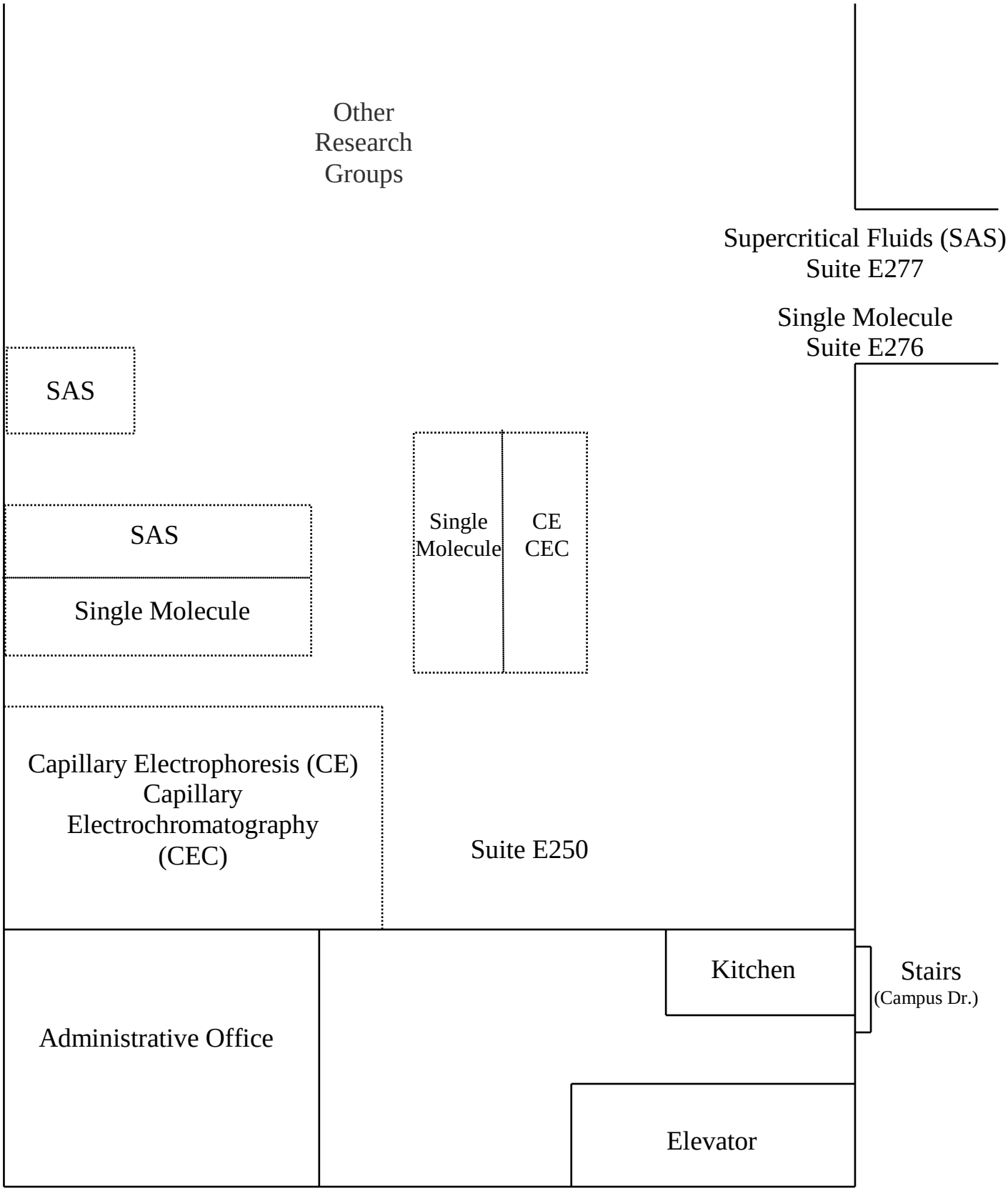

CLARK CENTER, EAST WING

STANFORD CAMPUS MAP

ZARELAB (West)
J.H. Clark Center
318 Campus Drive

ZARELAB
Mudd Chemistry Bldg
333 Campus Drive

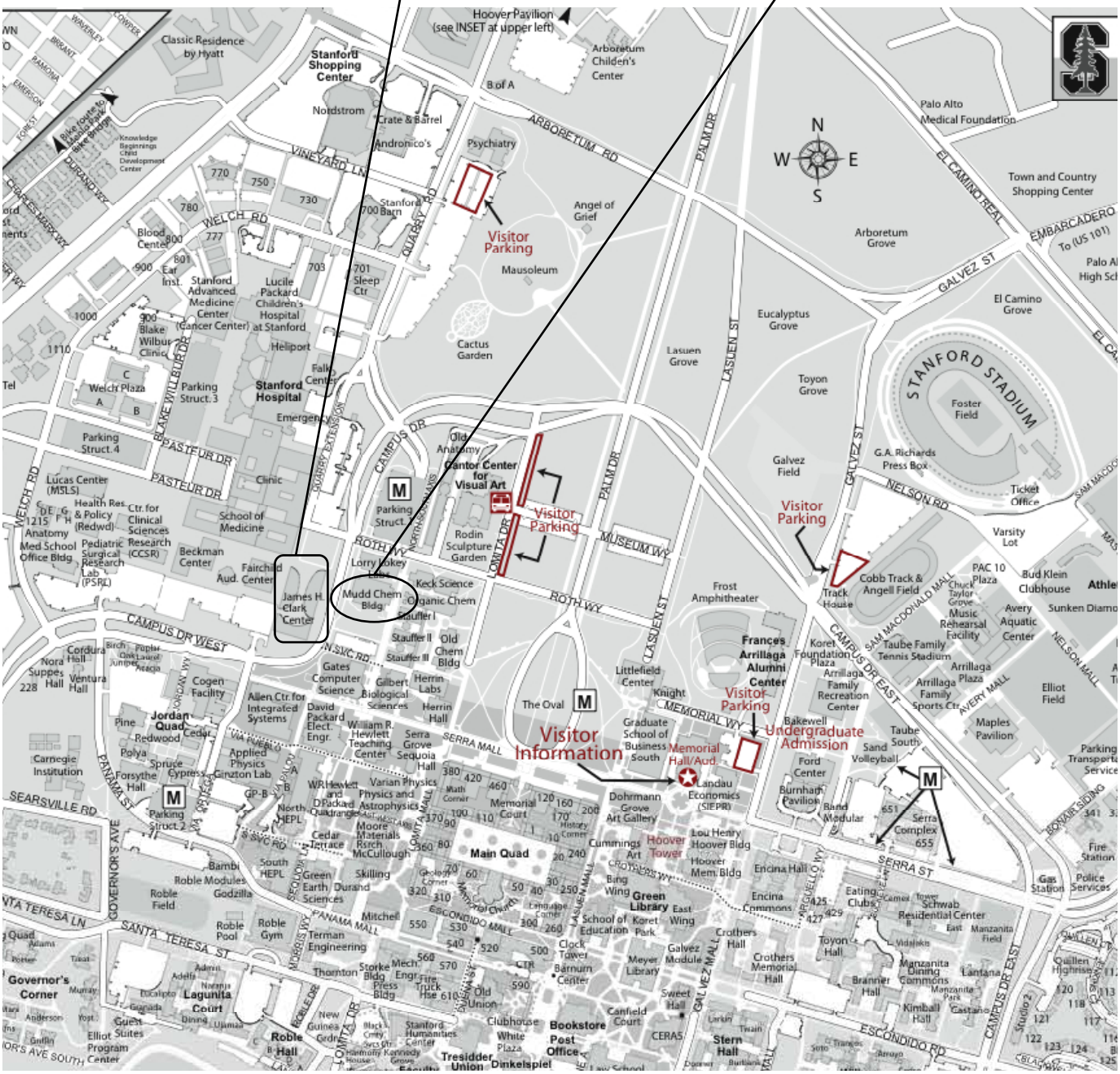

STANFORD VICINITY

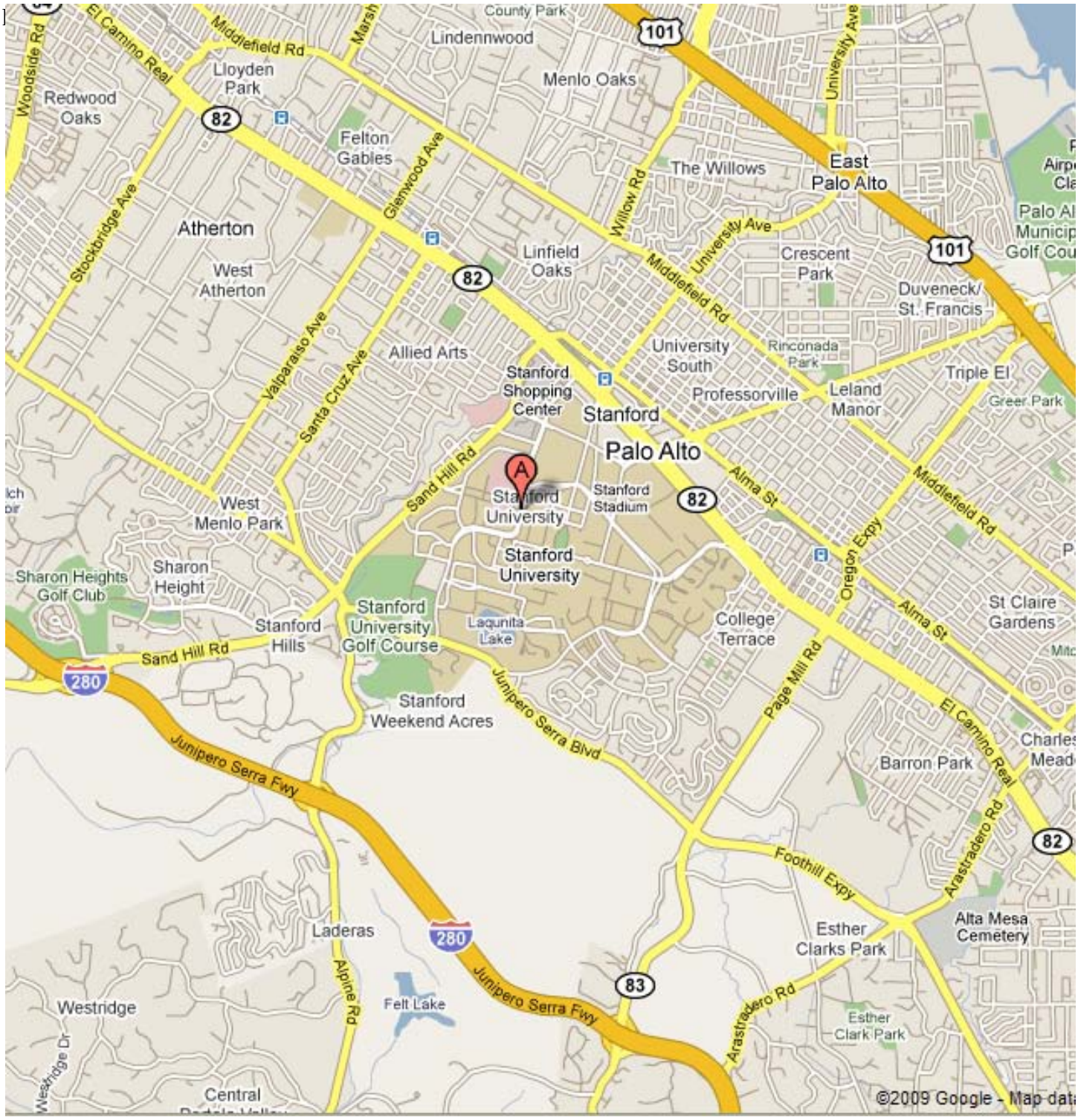

NOTES